Marine Pollution Bulletin 184 (2022) 114178

Contents lists available at ScienceDirect

Marine Pollution Bulletin

journal homepage: www.elsevier.com/locate/marpolbul

Acoustic characterisation of unexploded ordnance disposal in the North Sea using high order detonations

Stephen P. Robinson [a,*], Lian Wang [a], Sei-Him Cheong [a], Paul A. Lepper [b], John P. Hartley [c], Paul M. Thompson [d], Ewan Edwards [e], Michael Bellmann [f]

[a] National Physical Laboratory, Hampton Road, Teddington TW11 0LW, UK
[b] Loughborough University, Loughborough LE11 3TU, UK
[c] Hartley Anderson Ltd, Aberdeen AB11 5BE, UK
[d] Lighthouse Field Station, School of Biological Sciences, University of Aberdeen, Cromarty IV11 8YL, UK
[e] Marine Scotland Science, Marine Laboratory, 375 Victoria Road, Aberdeen AB11 9DB, UK
[f] Institute for Technical and Applied Physics GmbH, Marie-Curie-Straße 8, D-26129 Oldenburg, Germany

ARTICLE INFO

Keywords:
UXO
Explosion
Acoustic
Noise
Pollution

ABSTRACT

Results are presented of acoustic measurements made during the disposal of 54 items of unexploded ordnance (UXO) in the North Sea during the pre-construction phase of two offshore windfarms. The disposals were conducted using high-order controlled detonation of donor charges placed on the seabed adjacent to the UXOs. The total charge masses ranged from 2.5 kg to 295 kg TNT equivalent, and acoustic measurements were made at ranges of 1.5 km to 58 km from the UXO. High-order detonations can present a risk of injury or death to marine mammals and other fauna from the high sound levels produced, and these results represent the largest data set of acoustic measurements ever assembled for publication. Acoustic measurements were also made on small scare charges, used as mitigation. The sound pressure pulses are presented with their spectra, and the levels of peak sound pressure and sound exposure are presented as a function of range from the source. Measured levels are compared to data from a shallow-water propagation model, and to widely-adopted exposure level thresholds used for marine mammals, illustrating the potential for injury at distances of several kilometres.

1. Introduction

The seabed of North West European waters contains much unexploded ordnance (UXO), posing a hazard to offshore developments such as offshore windfarms. The location and spatial scale of many windfarm developments and cable and interconnector projects means there is a high potential to encounter UXO during construction, particularly where there is overlap with World War I and World War II conflict areas, military training areas and munitions disposal sites (Davies, 1996; Detloff et al., 2012; Eitner and Tröster, 2018). When UXO cannot be avoided or safely removed, explosive ordnance disposal (EOD) is necessary. The favoured disposal method has traditionally been to use a high-order controlled detonation conducted by exploding a donor charge placed adjacent to the UXO munition (Cooper, 1996; Sayle et al., 2009; Albright, 2012; Aker et al., 2012; Cheong et al., 2020). These disposals produce acoustic pulses, which can make significant contributions to the soundscape over a wide area (Sertlek et al., 2019; Merchant et al., 2020), and can have a number of adverse environmental consequences, one of which is the risk to marine fauna from exposure to the high amplitude sound levels produced (Yelverton et al., 1973; Ketten et al., 1993; Dahl et al., 2020; Todd et al., 1996; Finneran et al., 2000; Danil and St. Leger, 2011; Sundermeyer et al., 2012; von Benda-Beckmann et al., 2015; Parsons et al., 2000; Salomons et al., 2021, Siebert et al., 2022).

Impulsive sounds of very high amplitude also present challenges for effective mitigation, with potentially large exceedance areas for commonly-used exposure thresholds (Finneran and Jenkins, 2012; Popper et al., 2014; NMFS, 2018; Southall et al., 2019). Common mitigation strategies involve the use of spatial and temporal restrictions on the activity, visual and passive acoustic monitoring, and the introduction of additional noise of lower amplitude to create an aversive reaction by use of Acoustic Deterrent Devices (ADDs), and by use of small "scare" charges (JNCC, 2010; Merchant and Robinson, 2020). Noise abatement technologies have also been employed including the use of bubble

* Corresponding author.
E-mail address: stephen.robinson@npl.co.uk (S.P. Robinson).

https://doi.org/10.1016/j.marpolbul.2022.114178
Received 18 May 2022; Received in revised form 22 September 2022; Accepted 23 September 2022
Available online 4 October 2022
0025-326X/© 2022 The Authors. Published by Elsevier Ltd. This is an open access article under the CC BY-NC-ND license (http://creativecommons.org/licenses/by-nc-nd/4.0/).

curtains to attenuate the radiated sound (Loye and Arndt, 1948; Domenico, 1982; Schmidtke, 2010; Schmidtke, 2012; Croci et al., 2014; Merchant and Robinson, 2020). In recent years, there has been a focus on alternative methods of disposing of UXO (Koschinski, 2011; Koschinski and Kock, 2009; Koschinski and Kock, 2015) including the use of low-order techniques such as deflagration, a method that until recently has been more commonly used for military EOD operations where a small, shaped charge creates a plasma jet which penetrates the UXO casing and initiates a low-order combustion (Merchant and Robinson, 2020; ESTCP, 2002). Deflagration has been shown to produce substantially reduced levels of radiated sound in controlled experiments compared to high-order detonations (Robinson et al., 2020), but as yet such low-order techniques have been infrequently used offshore.

Although there is extensive literature on explosions as acoustic sources in the ocean, in general the sources in these studies have been suspended in the water column. The characterisation of UXO detonations presents additional difficulties because the condition of the ordnance itself can lead to a wide variation in apparent acoustic source level. The UXO will most likely be resting on the seabed and may be partially (or even fully) buried and, after up to 100 years in place, may exhibit substantial degradation of its physical structure (Cristaudo and Puleo, 2020). This means that it is not possible to be certain of the effective charge size (and therefore source level) for high-order detonations of UXO at sea. This uncertainty makes it difficult to draw definitive conclusions about measurements made on UXO disposals *in situ*. The most comprehensive recent study of the acoustics of high-order UXO detonation is by Salomons et al. (2021) where the opportunity was taken to record acoustic signals during disposal of two UXOs (of respective charge masses 325 kg and 140 kg, TNT equivalent) in the North Sea using three acoustic recorders at distances ranging from 1.5 km to 12 km. In the work, an explosive emission model was combined with a shallow-water propagation model. Measured and calculated noise levels were used to determine permanent-threshold-shift exposure ranges for harbour porpoises (*Phocoena phocoena*), with values obtained ranging from 2 km to 6 km.

To minimise the uncertainty in any measurements, it would be desirable to undertake a controlled experiment on ordnance of known charge size and status in a well-characterised offshore location. However, because of negative environmental impact of explosions, it is not justifiable to introduce additional ordnance into the marine environment for the purposes of scientific study, and use must be made of planned disposal campaigns for existing UXO. Therefore, the strategy adopted for the study reported here was to make use of measurements made during the licensed EOD operations for two offshore windfarms in UK waters: Moray East offshore windfarm and Neart na Gaoithe offshore wind farm (NnG). Acoustic measurements were made at ranges from 1.5 km to 58 km of high-order detonations on 54 items of UXO during the pre-construction phase of the two windfarms, with the estimated UXO charge masses ranging from <1 kg to 295 kg TNT equivalent using donor charges of between 2.5 kg and 25 kg. Measurements were also made of small scare charges of between 50 g and 250 g, used as acoustic deterrents as part of mitigation at the UXO clearances. The levels of peak sound pressure and sound exposure are presented as a function of range from the source. The measured levels are compared to data from modelling using a source model and shallow-water propagation model, enabling the range to be estimated for the exceedance of commonly used exposure level thresholds for marine mammals.

Although the authors recognise the interest and potential importance of measuring sound particle velocity and seabed vibration during UXO detonations, such measurements were not an option during the work reported here due to the lack of available instrumentation during the two UXO clearance campaigns.

In this paper, we describe the experimental configuration for the measurements at each windfarm, and the acoustic modelling approach. The results are presented, with a discussion of their significance and a comparison to other studies.

2. Experimental method

2.1. Locations and experimental configuration

Moray East is a 950 MW offshore windfarm located in the Moray Firth, off the north east coast of Scotland. The windfarm covers an area of 295 km^2 located a minimum of 22 km from shore with a 52 km offshore cable route. During the licensed EOD operations in March and April 2019, measurements were made during disposal of 17 UXO targets identified within the windfarm site and cable route. There was some uncertainty in the estimates of the charge sizes of the UXO, with a range of sizes provided by the EOD operators, and so the average (arithmetic mean) values were used in the analysis for this study. The estimated average charge sizes (in TNT equivalent) ranged from <0.5 kg to 295 kg, with the most common UXO type being designated as "22 to 60 kg" (average 41 kg) and with the two largest types (a torpedo and a "buoyant" sea mine) designated as 163 to 220 kg (average 201 kg) and 176 to 365 kg (average 295 kg). The EOD operations were undertaken using donor charges of between 1 kg and 25 kg. No noise abatement barrier techniques were used, but for mitigation before the EOD operation, ADDs were deployed followed by scare charges of increasing charge size, ranging from 50 g to 250 g. As part of this study, the acoustic signals from the scare charges were also measured, the scare charges being detonated at a depth of nominally 20 m at locations adjacent to the UXO position. Recordings were made using a total of 9 bottom-mounted acoustic recorders, positioned at ranges of between 5 km and 58 km from the UXO locations. Fig. 1 shows the locations of the windfarm, UXO and the acoustic recorders for the Moray East campaign.

The NnG offshore windfarm is located 15.5 km off the Fife coast and covers an area of approximately 105 km^2. During the licensed EOD operations from May to July 2020, measurements were made during disposal of 37 UXO targets that had been identified within the windfarm site and cable route. In total, 27 of the UXO were identified as naval artillery shells having estimated effective charge sizes (in TNT equivalent) of 102 kg (identified as "15-in. projectiles") and with the range of charges sizes spanning 0.1 kg to 102 kg. The EOD operations were undertaken using donor charges of either 2.5 kg or 5 kg. Once again, though no noise abatement barrier techniques were used, for mitigation before the EOD operation both ADDs and scare charges of increasing size were deployed, the sizes being 50 g, 100 g and 150 g. Again, as part of this study the acoustic signals from the scare charges were also measured, the scare charges being detonated at a nominal depth of 20 m at locations adjacent to the UXO. Recordings were made using a total of 4 bottom-mounted acoustic recorders, positioned to the north of the UXO cluster at ranges of between 1.5 km to 35 km from the UXO locations. Fig. 2 shows the locations of the windfarm, UXO and the acoustic recorders for the NnG campaign.

As far as possible, the measurement procedure followed the protocol defined by the Offshore Energy Strategic Environmental Assessment programme, part of the UK Department for Business, Energy and Industrial Strategy (BEIS, 2020), based on the procedures described in NPL Good Practice Guide 133 (Robinson et al., 2014) and ISO 18406 (ISO 18406:2017, 2017), the latter originally intended for measurement of marine pile driving. The protocol requires that at least four measurement positions be used, at four range categories of: 1 km to 3 km, 3 km to 5 km, 6 km to 8 km and ≥10 km. Although positioning recorders along specific transects for each individual UXO would be ideal, this is rarely practical when making measurements alongside a real-world EOD operation over the spatial scale of a windfarm and cable connector route. Where there is a large cluster of UXO targets over an area, the protocol allows for a number of recorders to be positioned at a variety of ranges and bearings in the region surrounding the UXO clusters, the recorders being left in place for the duration of the operations. This more practical arrangement was by necessity adopted for the work reported here.

A comparison between Fig. 1 and Fig. 2 shows that the bathymetry for the two windfarms areas is slightly different. The variations of

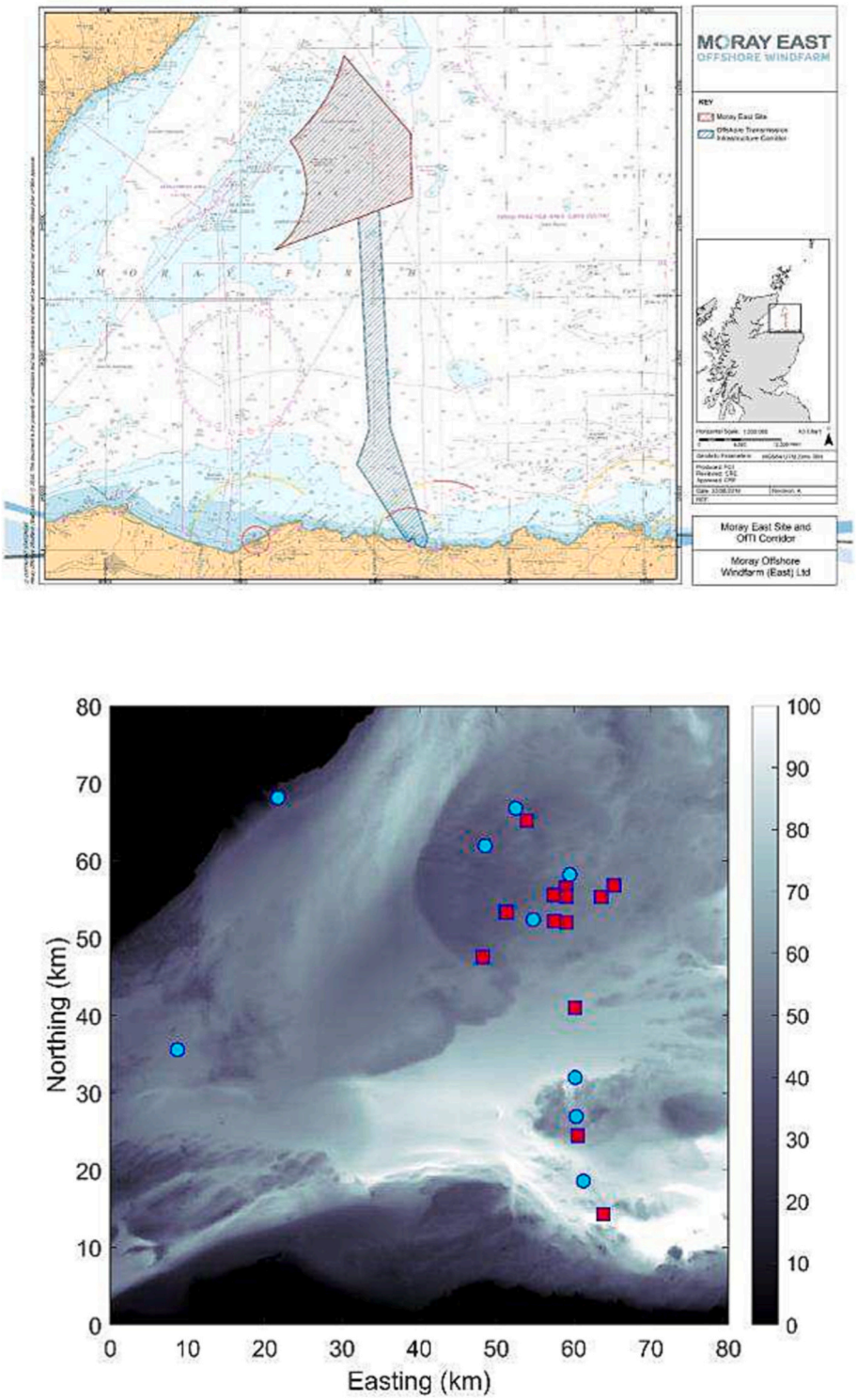

Fig. 1. Map of windfarm location (above) and bathymetric map (below) showing location of the UXO (squares) and recorders (circles) for Moray East (depth scale in metres).

bathymetry around the windfarm sites are minimal, but much greater variation exists along the cable routes to shore. The average water depth around the windfarm sites is about 45 m for Moray East site, and 50 m for NnG. The water depths for the cable route at Moray East approaches 100 m toward the south of the area.

2.2. Measurement instrumentation

For Moray East, seven Sound Trap ST300 recorders (manufactured by Ocean Instruments) with 16-bit resolution, and sampling rate of at least 48 kHz were deployed by the University of Aberdeen at selected positions. The systems had a usable bandwidth from 10 Hz to at least 20 kHz and with a maximum detectable sound pressure of 575 Pa (175 dB re 1 μPa). In addition, two DSG-ST recorders with 16-bit resolution and

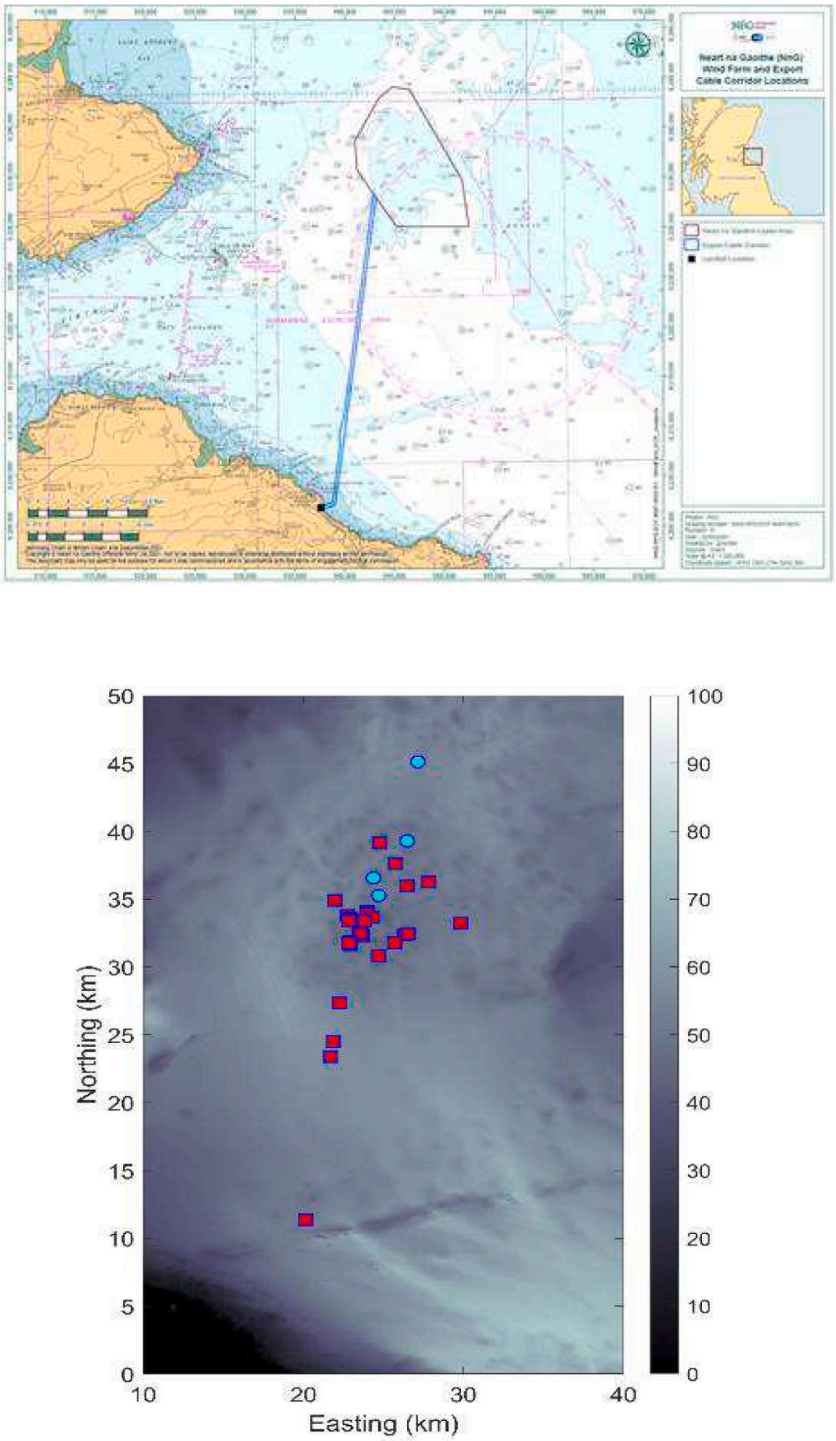

Fig. 2. Map of windfarm location (above) and bathymetric map (below) showing location of the UXO (squares) and recorders (circles) for the NnG site (depth scale in metres).

bandwidth of 10 Hz to 20 kHz (manufactured by Loggerhead Instruments) were deployed by Marine Scotland at more distant westerly locations closer to the coast. All recorders were bottom mounted at a nominal height of 2 m above the seabed.

For the measurement campaign at NnG, four bottom mounted acoustic recorders manufactured by itap GmbH and consisting of a Teledyne Reson TC4033 hydrophone combined with a preamplifier and Marantz PMD 620 audio recorder (NnG, 2021) were deployed at the northern end of the UXO cluster. The recorders are identical to those used in other recent UXO studies (Salomons et al., 2021) and used 16-bit resolution with a sampling rate of 44.1 kHz. These systems had a bandwidth of 10 Hz to 20 kHz, and were less sensitive than the devices used for Moray East, with the maximum detectable sound pressure set to either 25 kPa (208 dB re 1 μPa) or 158 kPa (224 dB re 1 μPa).

The measurements for Moray East were in some respects opportunistic, with the recordings of UXO detonations being made with recorders that had been deployed in strategic positions to detect sound from a number of different sources in the area. For a given UXO,

recorders at locations close to the UXO produced recordings which were saturated (clipped) due to the high amplitude of the signals received, and these recordings were not used. Although loss of data due to saturation prevented valid measurements being made at ranges closer than 13 km, measurements were possible at ranges of up to 58 km. Data loss through clipping happened less often for the NnG campaign where recorders of lower system sensitivity (and higher maximum detectable sound pressure) were used, enabling measurements to be made in the range from 1.5 km to 30 km.

The recorded data for the acoustic pulses were analysed and two acoustic metrics were calculated: peak sound pressure in MPa (sometimes referred to as the zero-to-peak sound pressure) and its level in dB re 1 μPa; and the sound exposure level (SEL) in dB re 1 $\mu Pa^2 s$ calculated both as a broadband value and in decidecade bands (one third octave bands calculated using base 10 [ISO 18405]). The focus was on these metrics because they are key to the calculation of exposure for certain classes of marine mammals (Southall et al., 2019; NMFS, 2018; Popper et al., 2014). The definitions of these terms were adopted from ISO 18405 (ISO 18405:2017, 2017), with the calculations on the acoustic pulse following the procedure described in the protocol (BEIS, 2020).

3. Acoustic modelling

3.1. Modelling approaches for explosive sources

Underwater explosions as sources of sound have been the subject of considerable scientific study since the 1940s, both theoretically and experimentally (Cole, 1948; Arons, 1954 and 1970; Weston, 1960). The models developed in the above papers for deep water have been shown to agree reasonably well with experimental characterisation of explosive sources in shallow water environments (Gaspin and Shuler, 1972; Gaspin et al., 1979; Chapman 1985& 1988; Hannay and Chapman, 1999; Soloway and Dahl, 2014; Wiggins et al., 2019), but there are limited experimental data available to describe shallow-water propagation over considerable distances for these sources (Salomons et al., 2021), and few estimates of the acoustic output from explosive sources positioned on or below the seabed, one exception being for offshore decommissioning (NOAA, 2016).

In an explosion, the chemical chain-reaction occurs at supersonic speed producing a high amplitude acoustic pulse which propagates nonlinearly in the form of a shock-wave which reaches out to a range of about 10,000 times the charge radius (Cole, 1948; Weston, 1960). Beyond this range, the propagation may be considered linear, and use can be made of conventional linear propagation models and metrics such as energy source level (ISO 18405:2017, 2017).

In this study we used an empirical model for energy source spectra of UXO detonations which was developed in a previous study (Robinson et al., 2020) and which closely follows those in the literature (Arons, 1954; Weston, 1960). The energy source level (ESL) spectrum for a specific charge size was then used with a shallow-water propagation model based on wave-number integration to calculate the Received Level spectrum (RL) at a receiver location through the relation RL = ESL – PL where PL is the propagation loss calculated with the model. The peak sound pressure was then calculated from the RL spectrum using an inverse Fourier transform.

3.2. Source modelling

The acoustic signal from unbounded underwater explosion consists of a shock-wave as a rapid pressure rise to a pressure peak, and followed by an exponential decay of the pressure, then a number of bubble oscillations. The detonation of UXOs is different because they all sit on the seabed, or are buried (partially or fully). One effect of the seabed on the bubble oscillation is that the seabed prevents the formation of a truly spherical bubble, resulting in a reduction of the peaks associated with the bubble oscillations.

To simplify the modelling of the impulsive acoustic signal propagation in this study, the bubbles are ignored so only the shock-wave is considered as an acoustic source. This simplification will not affect the prediction of the peak of the pulsed waveform since the bubbles do not contribute to the impulse peak. However, a slight reduction of SEL can be expected if the contribution from the bubbles is ignored. In the previous study, the SEL of the bubble pulse was typically 8 dB lower than for the main pulse.

The shock wave signal was synthesised based on waveforms measured in previous studies at close range (Robinson et al., 2020). The empirical fit to the acoustic pulse was used to generate the source spectra shown in Fig. 3 for a selection of donor and scare charge sizes. The shock wave signal is highly non-linear at close range and approaches linear over distances of the order 10^4 times the charge radii (Arons, 1970; Ainslie, 2010). For the work here, we used the above to scale the shock wave spectrum as the source spectrum for modelling. It should be noted that the 2020 work used modern plastic explosive (PE4) which is different to the type of explosive found in older UXO and this is a source of uncertainty in the source model. However, the 2020 study showed good agreement with existing models and so this uncertainty is not considered significant.

3.3. Modelling of propagation

Propagation of the impulsive signals generated by the underwater explosions was modelled with the OASES propagation model (Schmidt and Jensen, 1985), a model that uses a wave-number integration method for acoustic propagation within stratified media (Jensen et al., 1997). This was combined with signal spectrum of the empirical model of the explosive signal at source. The OASES model can be applied for layered media and include shear wave properties. This is useful if the seabed consists of a thin layered sediment over a bedrock basement layer. The time domain signal for the simulation was then synthesised with the frequency domain signal *via* inverse Fourier transform. Estimates of both peak sound pressure level and SEL can be obtained from this analysis.

The input parameters used for the propagation modelling are listed in Tables 1 and 2 for Moray East and Neart Na Gaoithe sites respectively. The sites are all shallow water with typically sandy seabed (SEA5, 2004; Moray East, 2011; NnG, 2012). At the Moray East site, a thin layer of gravelly sand with an average thickness of about 2 m exists above layers of tills of up to 70 m, with a sandstone basement layer. At the NnG site, there is a sand layer of mean thickness of 12.9 m above a limestone basement. There are variations of bathymetry around the windfarm footprints, but much greater variation occurs along the cable routes to shore, the average water depth around the windfarm sites being about 45 m for Moray East, and 50 m for NnG. The acoustic source in the model was positioned on the seabed at the location of the UXO (the source

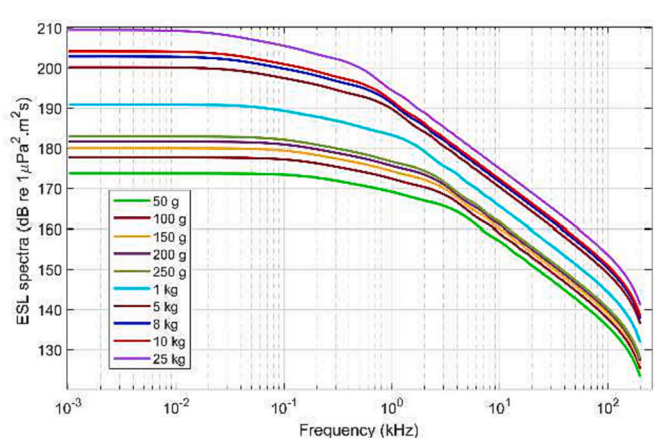

Fig. 3. Energy source level spectral levels used for a variety of charges sizes.

Table 1
Parameters used for propagation modelling in Moray East.

Property		Water	Sediment layer 1	Sediment layer 2	Base layer
Sound speed (ms^{-1})	c_p	1481.9	1780.2	1565	3300
	c_s	N/A	N/A	N/A	1941.2
Density (gcm^{-3})		1	2.034	1.596	2.5
Atten. (dB/λ)	A_p	[Skretting & Leroy]	0.3	0.2	1.06
	A_s	N/A	N/A	N/A	1.56
Layer thickness (m)		45	2	70	Infinite

Table 2
Parameters used for propagation modelling at NnG.

Property		Water	Sediment layer	Base layer
Sound speed (ms^{-1})	c_p	1482.3	1697.2	3500
	c_s	N/A	N/A	1842.1
Density (gcm^{-3})		1	1.94	2.45
Atten. (dB/λ)	A_p	[Skretting & Leroy]	0.2	1.06
	A_s	N/A	N/A	1.56
Layer thickness (m)		50	12.9	Infinite

depth being set equal to the water depth).

The acoustic properties of the sediments in Tables 1 and 2 are described with Hamilton's model (Hamilton, 1980). The acoustic properties of the bedrock basement layers are taken from (Winkler and Murphy, 1995). An *in-situ* measurement of sound speed at NnG revealed weak negative sound speed profiles in the water columns, with an average sound speed of 1482.3 ms^{-1} (NnG, 2021). For Moray East, the average sound speed in the adjacent area of the North Sea for April of 1481.9 ms^{-1} was used. The underwater channels were considered as horizontally stratified with a constant sound speed and density in each of the layers. The attenuation in the water was obtained from (Skretting and Leroy, 1971).

3.4. Frequency bandwidth versus range

The sound radiated from explosions contains high frequency components, with signal bandwidth extending up to hundreds of kilohertz. This presents serious challenges for modelling acoustic propagation over large ranges due to the computational time required. The peak sound pressure is the metric most affected by a restriction in model bandwidth. To examine this, the effects of model bandwidth on signal peak were examined by use of a variety of bandwidths applied to the measured and modelled signals at different ranges. The results demonstrated that use of a maximum frequency of 2 kHz for the acoustic modelling led to reduction of the level of the peak sound pressure of around 0.5 dB at ranges >10 km. Therefore, the 2 kHz bandwidth was applied to propagation modelling at ranges >10 km, while a larger bandwidth of 20 kHz was applied to ranges from the source of up to 2 km, and 8 kHz bandwidth from 2 km to 10 km respectively. Note that, for the analysis of the experimental data, the full signal bandwidth available was used. Note that the levels were generally above ambient levels for frequencies below 2 kHz, but this was not generally true for highest frequencies and the greatest ranges (see Fig. 16).

4. Results

4.1. Broadband results for high-order UXO detonations

The broadband SEL values (unweighted) *versus* range for the UXO detonations at Moray East are shown in Fig. 4 for the various charge sizes. In the figure legend, the average of the estimated charge sizes for each UXO are stated along with the donor charge, the maximum UXO

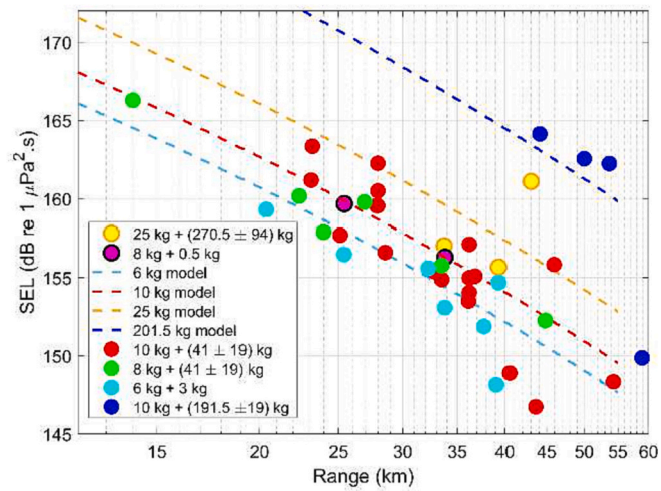

Fig. 4. The broadband SEL values *versus* range at Moray East for the various charge sizes. Also shown are the model predictions for four of the charge sizes.

size being 270.5 kg ± 94 kg with a donor charge of 25 kg. Note that because the UXO locations vary (but the seven recorder positions are fixed), the ranges for the measurements are not closely grouped but vary widely (the recorders are at different ranges and along different bearings for each UXO). The "clipped" recordings were not analysed. Also shown in Fig. 4 are the model predictions for a charge size of 201.5 kg, and three of the donor charge sizes: 6 kg, 10 kg and 25 kg. The agreement between the model prediction and the measured values is highly variable, with the latter in many cases being lower than the predictions. In some cases, the measured values agree reasonably well with the levels expected for the donor charge alone, a good example being the 8 kg donor charges where the levels fall between the model for 6 kg and 10 kg irrespective of the UXO charge size. However, for the 10 kg + 191.5 kg combination, the measured levels are much higher than for the donor charge alone, suggesting UXO detonation.

Fig. 5 shows the level of the peak sound pressure ($L_{p,pk}$) for the same measurements made at Moray East, with the same conventions of symbols and legend. The model here appears to overestimate the peak sound pressure by typically around 3 dB to 5 dB (though occasionally by as much as 10 dB), with the majority of the model results lying above the level of the measured data. The variations of modelled peak pressure level along the range are caused by the dispersive effects of the sound propagation in this underwater channel where the seabed consists of a number of layers on top of rock basement.

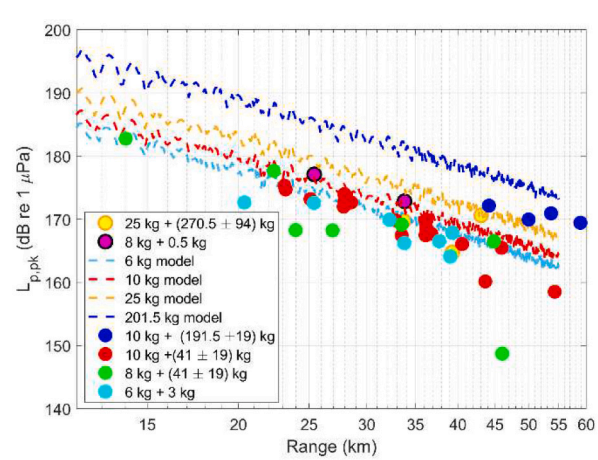

Fig. 5. The level of the peak sound pressure *versus* range at Moray East, with the selected model predictions.

Fig. 6 shows unweighted broadband SEL values *versus* range for the UXO detonations at NnG. Here, for 25 of the 37 UXO recorded, the UXO charge size was 102 kg and a 5 kg donor charge was used for the high-order detonation (data shown in orange). There were also 7 smaller UXO detonated using a 5 kg charge, and three very small value UXO where a 2.5 kg charge was used (blue data).

Once again, the ranges for the measurements are not closely grouped because the four recorders are at different ranges and along different bearings for each UXO. Here, measurements were possible at closer ranges without loss of data due to clipping. Also shown in Fig. 6 are the model predictions for the two donor charge sizes used. In general, the SEL values exceed the predictions for the donor charge alone, but do not exceed the prediction for the total charge size of 107 kg.

Fig. 7 shows the level of the peak sound pressure ($L_{p,pk}$) for the NnG measurements, with the same conventions of symbols and legend. As for the SEL, the levels exceed those of the donor charge alone but are lower than predicted for the total charge size of 107 kg.

4.2. Broadband results for scare charges

The scare charges used as mitigation were also measured for both Moray East and NnG. Fig. 8 shows the broadband SEL values *versus* range for the 50 g, 100 g and 150 g scare charge detonations at NnG. Also shown is the predictive model for charges of these sizes with the source suspended at depths of 20 m.

It is clear that there is substantial variation in the measured data for a scare charge of a given size measured at a similar range from the source, with variations of between 2 dB and 6 dB evident. It should be remembered that measurements made at similar ranges from the source are for different UXO detonations and likely to be along different transects at different bearings from the source, such that both variations in the source output and the propagation will contribute to the scatter in the results (and the deviations from the predictive model). In general, the higher the charge size, the higher the received SEL, but the agreement with the model in general degrades with increasing range.

Fig. 9 shows the level of the peak sound pressure for the scare charge measurements made at NnG, with the predictive model for charges of these sizes. Significant scatter is observed in the results for a given range and scare charge (for example, >10 dB at 2.5 km for the 150 g charge). In general, the higher the charge size, the higher the received peak sound pressure. The agreement with the model is slightly better than for the SEL, but again there is a model over-prediction at the highest ranges.

Fig. 10 shows the broadband SEL values *versus* range for the scare charge detonations at Moray East, the sizes being 50 g, 100 g, 150 g, 200 g and 250 g. Also shown is the predictive model for three of the charge sizes (again assuming the source is at a depth of 20 m). Notice that the axis scales for the range are different to those for Figs. 8 and 9.

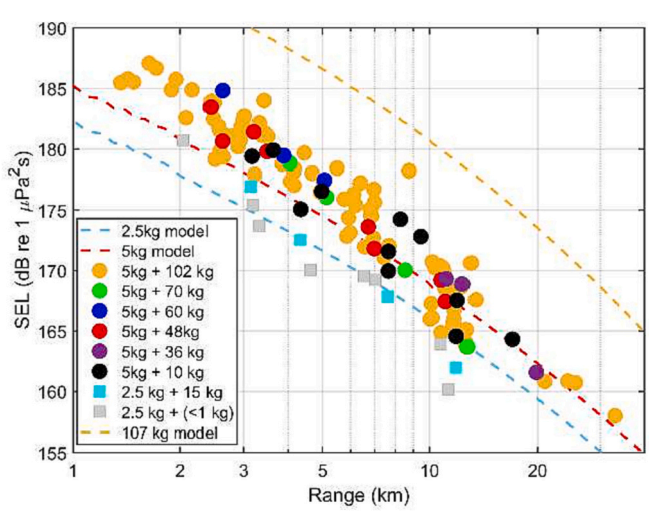

Fig. 6. The broadband SEL values *versus* range at NnG for the various charge sizes, with model predictions for the two donor charge sizes.

In this case, the scatter in the results increases with range, with typically 3 dB to 4 dB variation at lower ranges increasing to up to 10 dB at 50 km. In general, the relation between the charge size and the received SEL is hardly evident, with the measured data clustered around the model prediction for the 50 g charges. It is unlikely that the predictive model overestimates the sound radiation substantially (this is not observed for the NnG UXO detonations) and it appears that the effective size for the many of the scare charges is lower than expected.

Fig. 11 shows the Moray East results for level of the peak sound pressure for the scare charges, again with the predictive models. Significant scatter is observed in the results for a given range and scare charge (for example, 12 dB at 25 km for the 50 g charge), and the relation between the charge size and the received SEL is again hardly evident, with the data agreeing well with the prediction for the 50 g charges.

4.3. Acoustic waveforms and spectra

The measured signals were analysed in the frequency domain by calculating the spectra in decidecade bands (these bands are "one-tenth decade bands" following the definition in ISO 18405 and are approximately equal to one-third of an octave). Fig. 12 shows the measured SEL decidecade spectra at 24 km for 5 kg donor charge and 102 kg UXO for NnG. Also shown are the modelled SEL spectra for both the 5 kg donor charge alone, and the 107 kg combination of donor and UXO.

In the case shown, the measured decidecade levels at frequencies above 100 Hz are closer to the model values for the donor charge alone, as is evident from the broadband data. It is also evident that the model underestimates the spectral levels at frequencies below 100 Hz, and particularly below 50 Hz. This is almost certainly due to inaccuracies in representing the seabed properties at low frequencies, a problem that has been reported in a number of recent noise mapping studies in the North Sea region (Binnerts et al., 2019; Kibblewhite, 1989).

Examples of the acoustic waveforms are shown in Fig. 13 for one of the 102 kg UXO (5 kg donor) at a range of 5.1 km at NnG, and for the 191.5 kg ± 19 kg UXO (10 kg donor) at 44.1 km for Moray East.

At the measurement distances and water depths that pertain here, it is not possible to view the direct acoustic signal in the absence of reflected signals from the surface and seabed. The bubble pulse that generally follows the main acoustic shock (typically by around half a second) is in general not resolved as a separate pulse in the data measured at large propagation ranges, and the bubble pulse is suppressed somewhat by the water depth and the proximity of the seabed. An example of a low frequency seismic precursor signal is just visible for the 5.1 km waveform (these signals can arrive before the water borne signal because of the higher sound speed in the seabed but are strongly low pass filtered by the absorption in the seabed).

Although the acoustic signals are recognisable as impulsive in nature even to ranges of up to 58 km, the pulse duration is seen to increase with range. The dilation of the acoustic pulse is initially due to the reverberation in the water channel, and at greater ranges is compounded by the dispersive nature of the propagation in a shallow water channel and by reflections from deeper layers beneath the seabed (Jensen et al., 1997). This dilation of the acoustic pulse as it propagates is evident from the increase in pulse duration apparent from Fig. 14 which shows the pulse length *versus* range for all 27 of the 102 kg UXO (5 kg donor) at NnG. The data for the individual recorders are shown in different colours, each being at a slightly different bearing (which contributes to the variation observed).

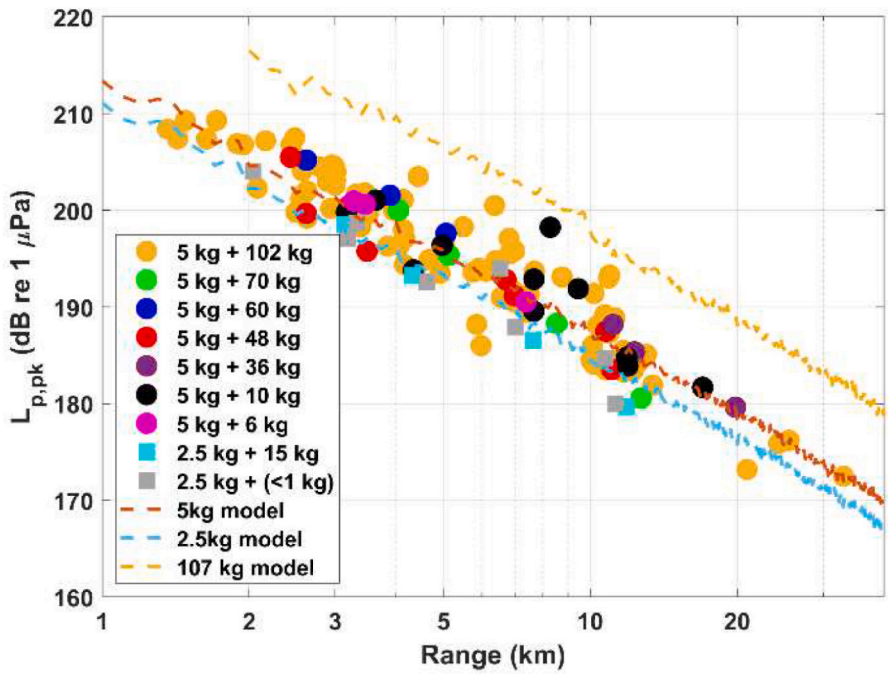

Fig. 7. The level of the peak sound pressure *versus* range at NnG for the various charge sizes, with model predictions for the two donor charge sizes.

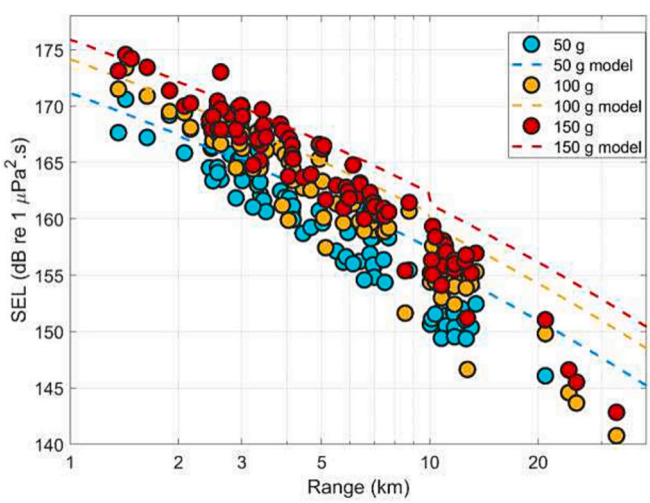

Fig. 8. The broadband SEL values *versus* range at NnG for the scare charges, with model predictions.

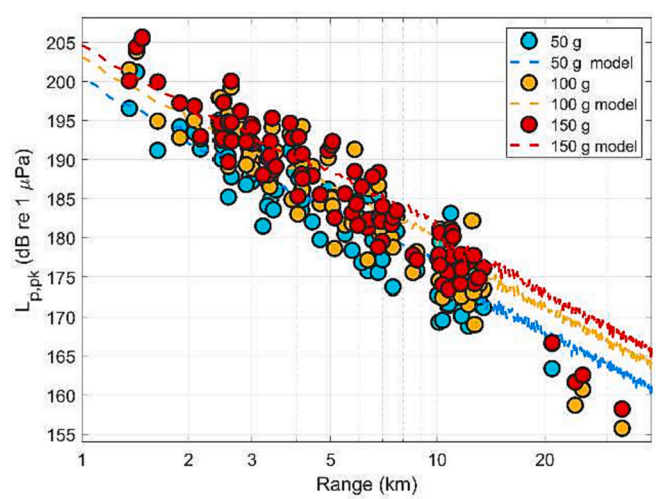

Fig. 9. The level of the peak sound pressure *versus* range at NnG for the scare charges, with model predictions.

5. Discussion

5.1. Features in the data

The measurements reported here show a considerable variation in received levels for both UXO and scare charges, even for similar charge size at a roughly equivalent range. For the wider variety of UXO size at Moray East this might be expected, but significant variation is also present at NnG where many of the UXO are nominally identical. There are several factors influencing this variation. The calibration of individual recorders is unlikely to play a significant role because the calibration uncertainties are typically of the order of 1 dB (Hayman et al., 2015; Hayman et al., 2017), considerably less than the variation observed. A malfunctioning or damaged recorder is likely to show consistently biased results for all recordings made with it and no such bias was observed. The variation in measured levels will be influenced by the experimental configuration. In an ideal scenario, recorders would be positioned in a transect along a single bearing perhaps with some redundancy (multiple hydrophones) at some locations, and these would then be re-deployed along different transects for each UXO detonation (BEIS, 2020). This was not possible for these campaigns where some of the measurements were opportunistic. Instead, the recorders were in fixed positions throughout the campaigns, each recorder representing a single measurement along a different transect and bearing, with differences in propagation leading to variations in recorded levels even for similar ranges from the source. This factor is mitigated by the fact that over the windfarm footprint the bathymetry and seabed properties are reasonably constant (making the propagation along different transects roughly equivalent), though more variation might be expected due to deeper water at the highest distances and along the cable route. An example can be seen in Fig. 4 where the 58 km measurement for the 191 kg ± 19 kg UXO appears to have a much lower SEL value than expected

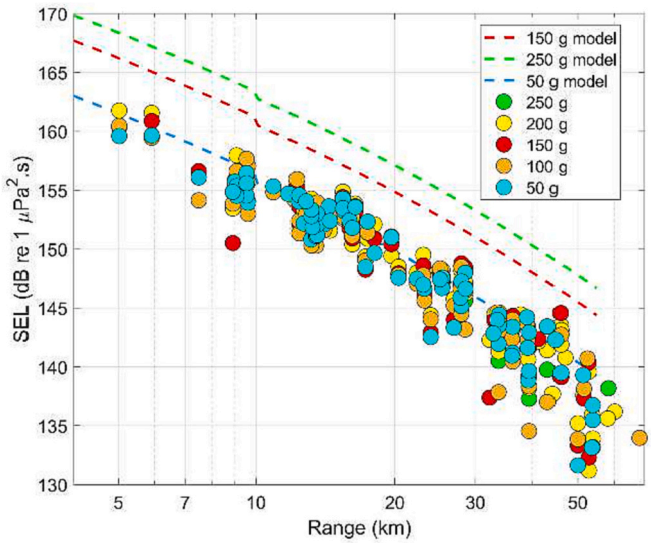

Fig. 10. The broadband SEL values *versus* range at Moray East for the scare charges, with model predictions.

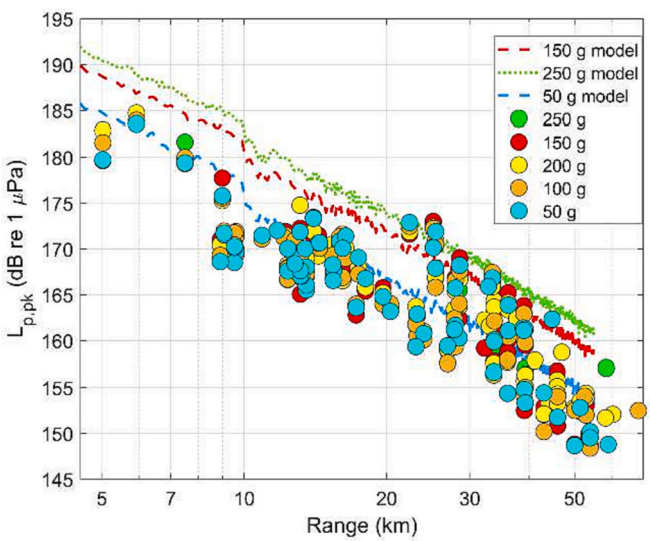

Fig. 11. The level of the peak sound pressure *versus* range at Moray East for the scare charges, with model predictions.

from the model (and differs markedly from the other measured data). Similar effects were reported by Salomons *et al* (2021). Inspection of the spectra shows that the SEL is reduced because much of the low frequency energy for the 50 km pulse has been attenuated due to the propagation path to this distant recorder (which includes bathymetric changes and variations of seabed properties that are not present for the other recorder positions). However, the level of the peak sound pressure (see Fig. 5) is less affected because the peak of the pulse is more dependent on the higher frequency content (which has been less affected by the low frequency propagation effects).

An additional factor is uncertainty in the effective net charge size for the UXO and donor charge combination. During EOD operations, estimates of UXO charge size may not always be accurate, and for Moray East only an estimated range of charge sizes was stated. It is also believed that some UXO targets contained little or no explosive (as might happen in the case of tracer shells). Furthermore, the condition of each UXO may vary with partial (or full) burial and different degrees of degradation, which affect the acoustic output. The donor charge may

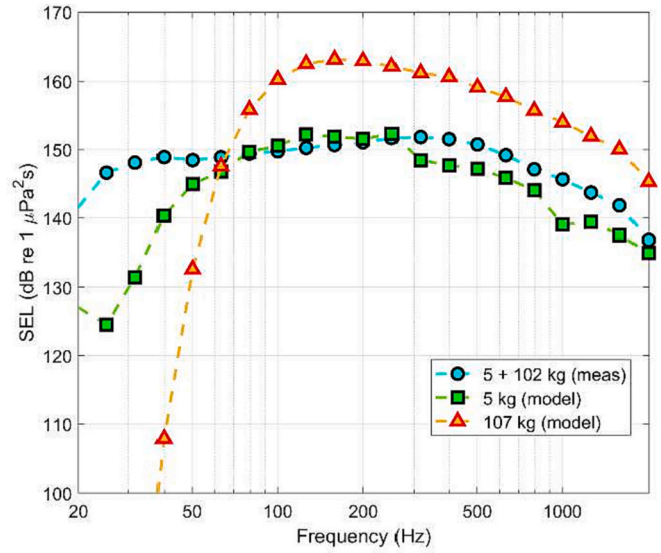

Fig. 12. Measured and modelled SEL decidecade spectra at 24 km for 5 kg donor charge and 102 kg UXO for NnG.

cause the UXO to only partially detonate or not detonate at all. That the above scenarios may have occurred in some cases is suggested by the fact that some of the detonations appear to generate levels more consistent with the donor charge alone.

Modelling and predicting the radiated sound from high-order UXO detonations is fraught with difficulty. The empirical models in the scientific literature were developed and validated for explosive sources suspended in the water column (Arons, 1954; Weston, 1960) and limited attempts have been made to model explosive sources on the seabed (NOAA, 2016; Salomons et al., 2021). Both the source model and the propagation contribute to the uncertainty. For the source model, the output is dependent on an accurate estimate of effective charge size. In addition, the partial burial of an acoustic source in the seabed affects the level of the sound radiated into the water column which decreases with increasing burial. This effect has been tested by running the acoustic model for a range of source burial depths, the results showing a reduction of up to 5 dB in SEL at 20 km for a 1 m burial. Note that modelling here is for an acoustic source, but the real source is actually a detonation on or just under the seabed. A validated theoretical or empirical model is not yet available for such explosive sources, where the detonation also causes considerable disturbance to the seabed, with considerable energy from the explosion expended in expelling the sediment in a large plume. For explosive sources suspended in the water column, the energy goes into heat and bubble creation in addition to the shock wave, but without the "muffling effect" of the seabed which absorbs some of the energy. The seabed is therefore likely to reduce the acoustic energy radiated compared to an explosion in mid-water. This partially explains why the levels recorded in this study and others are lower than might have been predicted by empirical models for mid-water explosions. A lack of full understanding of the mechanisms and influences involved in sound production for a seabed explosion mean that even when the mid-water empirical models are adapted for use with UXO as has been done here, the uncertainties involved mean that agreement between measurement and modelling may not be close. An additional factor which may reduce levels of radiated noise is cavitation shielding, as reported by Salomons *et al* (2021). In this process, bubbles are produced as the shock wave interacts with the pressure release water surface and cause increased attenuation in the sound propagation (von Benda-Beckmann et al., 2015). This affects sound paths at steeper angles more strongly than sound paths radiating horizontally into the water column, and it is difficult to quantify the effect for the results reported here. The fact that the model also overestimates for some of the scare charges may also be

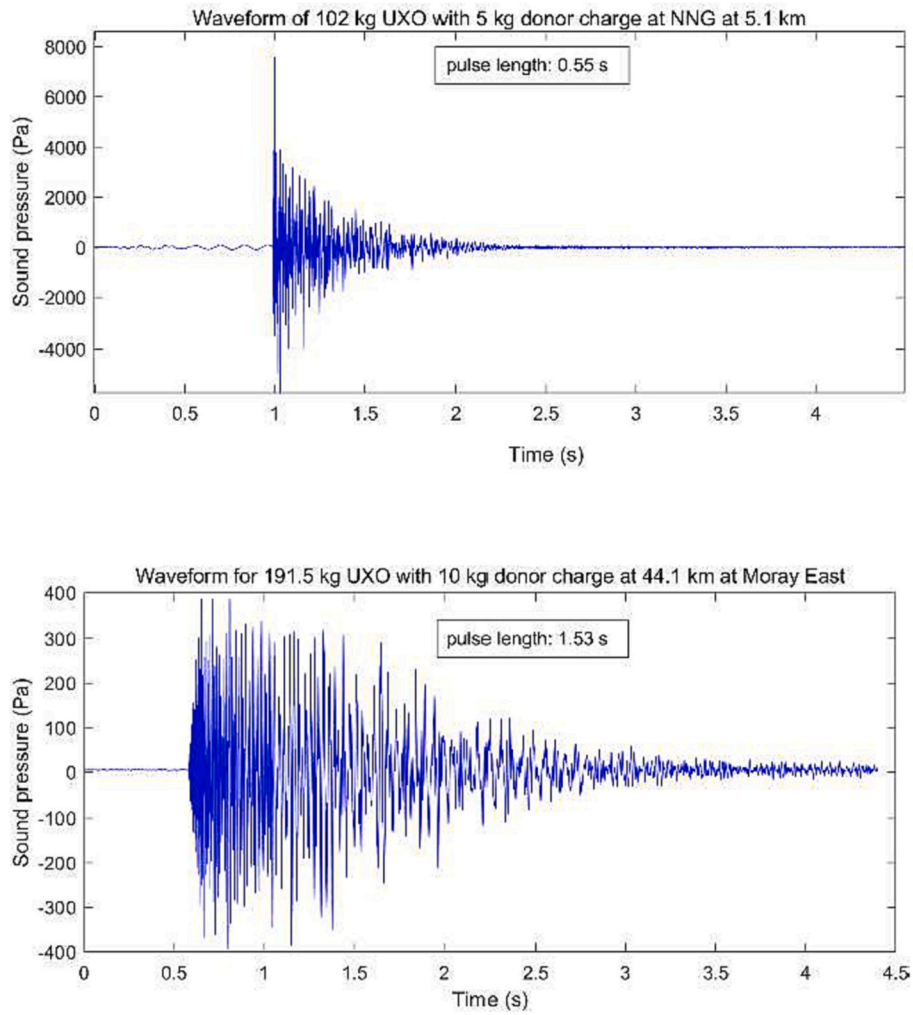

Fig. 13. Example waveforms for: 102 kg UXO with 5 kg donor charge at 5.1 km at NnG (top) and for a 191.5 kg UXO with 10 kg donor charge at 44.1 km at Moray East (bottom).

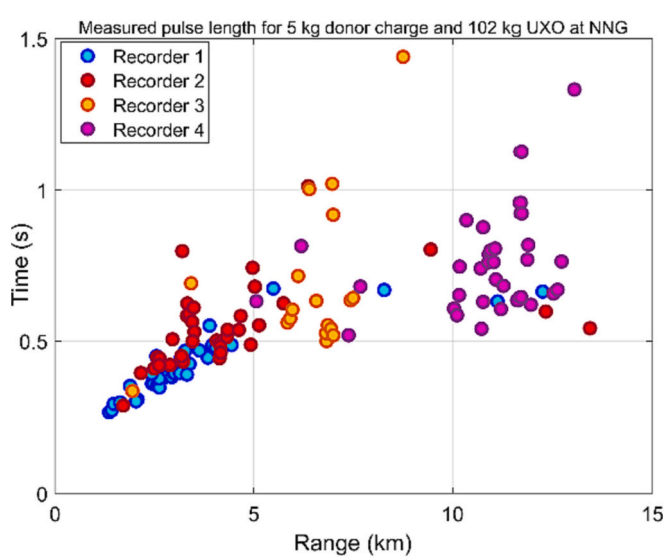

Fig. 14. Variation of measured pulse duration with range for 102 kg UXO and 5 kg donor charge at NnG (showing all four recorders).

evidence that cavitation shielding has some effect here.

The propagation modelling also suffers from uncertainty. Because it is not practical to model every possible transect from every UXO to every receiver location due to the computational time, an "average" propagation model to represent each windfarm site was developed. A more detailed model that accounts for spatial variations in the sediment properties and bathymetry would result in better agreement with the measured levels. This uncertainty is mitigated by the fact that the bathymetry and seabed properties were reasonably uniform for the windfarm sites, but inevitably this is a cause of discrepancies between the measured and modelled data. Additional uncertainties originate from the restricted upper frequency limit used for the model (2 kHz at ranges > 10 km compared to 20 kHz for the measurements). Finally, lack of knowledge of the properties of the seabed, especially the sound absorption, causes a significant uncertainty in the low frequency shallow water propagation. Any inaccuracies in the treatment of sound absorption would increase the discrepancies at high ranges from the source. This is a likely cause of the increasing underestimations observed in the modelled spectra compared to measurements at frequencies below 100 Hz and at the highest ranges (this uncertainty increases with range from the source) and contributed to some of the deviations shown at large ranges for Moray East (an example being the 58 km measurement for the 191 kg ± 19 kg UXO).

The measurement and modelling of the scare charges should not suffer from some of the above uncertainties because the explosions occur

in the water column rather than on the seabed, though the uncertainties in propagation modelling along different transects still applies. For NnG, the scare charge results show the expected higher levels for the larger charge sizes (with about 5 dB difference in SEL observed between the 50 g and 150 g charges) and the agreement with the modelling is quite reasonable (though degraded at higher ranges for the reasons mentioned above). For Moray East, the measured data do not seem to increase with charge size in the expected manner, with if anything less variation in received level even though a greater variety of nominal scare charge sizes were used. It is possible that some of this "compression" of the data may be due to the much greater ranges from the source that are apparent for measurements at Moray East. However, the data "appear" as if the scare charges were all of similar size (with the data clustered around the prediction for a 50 g charge), and it seems possible that this reflects the actual charge sizes used (the nominal charge size may not always be accurate). It is interesting to note that the received levels for the 50 g charge size are broadly comparable for both windfarm sites, for example SEL levels at 5 km are about 160 dB re 1 μPa^{2}s for both NnG and for Moray East.

The acoustic output of the scare charges is subject to additional uncertainty due to the fact that the process of firing the charges is not always scientifically controlled. For example, the exact location of the charge may be some distance away from the UXO site, and the nominal charge depth of 20 m may not always be correct. These factors can lead to variations in the measured levels at the recorder locations, and mean that the assumptions about locations and depth included in the source model may not always be valid.

The results of this study generally appear to confirm a number of the findings of Salomons et al. (2021) that modelling may overpredict the levels observed from UXO explosions. Certainly, the predictions from empirical scaling relations with respect to charge size suggest that errors can occur when one uses these relationships to predict peak sound pressure and SEL underwater explosions in shallow water at large ranges. The authors of Salomons et al., 2021 resolved the modelling issue by introduction of an empirical correction factor, but the maximum range in that study was 12 km. In the study reported here, the measurements are made over much greater ranges and it is therefore very ambitious to expect perfect agreement, especially out to ranges of >50 km.

An interesting observation on the results is the relationship between the peak sound pressure level and broadband SEL, a metric which has been described by other authors (Soloway and Dahl, 2014; von Benda-Beckmann et al., 2015). To examine this relationship, the level difference in decibels was calculated for all the recorded acoustic pulses from UXO detonations as a function of range from the source, with the results plotted in Fig. 15. The level difference between the two metrics decreases with range from the source, from over 20 dB at a few kilometres, to <10 dB at 55 km. This is as expected due to the increased propagation loss for higher acoustic frequencies (which have more influence on the peak sound pressure level).

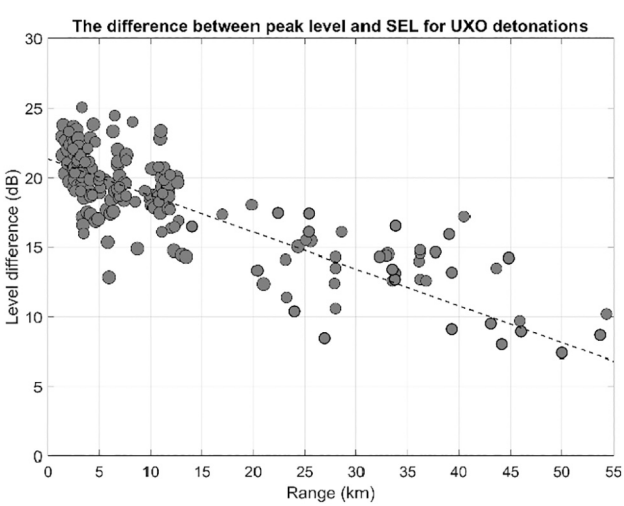

Fig. 15. Level difference for all the recorded acoustic pulses from UXO detonations as a function of range from the source. The gradient of the least squares linear fit is −0.26 dB/km.

5.2. Noise exposure

Fig. 16 shows the measured SEL decidecade spectra for the two waveforms shown previously in Fig. 13 at ranges of 5.1 km (for 102 kg UXO and 5 kg donor charge at NnG) and 44.1 km (for a charge of 191.5 kg and 10 kg donor charge at Moray East). Also shown are the background noise spectra illustrating that the highest frequencies of the measured signals are limited by ambient noise at the larger ranges (the noise limiting the measurements above the 8 kHz band for 44.1 km), whereas at 5.1 km the signal-to-noise ratio is good to up to the 16 kHz band. Also shown on the plot are the weighted spectra according to Southall et al., 2019 for the very high frequency (VHF) cetacean species (for example, the harbour porpoise, a key species in the North Sea). Although these criteria may be considered as current state-of-the-art, it is nevertheless worth noting that the criteria derived were not based on an extensive evidence base for explosive sources.

For three cetacean categories, Southall et al. (2019) gives PTS-based injury threshold levels, for example of 202 dB re 1 μPa for peak sound pressure level and 155 dB re 1 μPa^{2}s for weighted SEL for the VHF category. From an extrapolation of the modelled levels, the range for exceedance of the PTS injury threshold may be derived for the UXO charges. These are shown in Table 3 for all three species categories and for a variety of charge sizes, with exceedance values for PTS peak criteria in the range 1.6 km to 7.1 km for UXO of between 1 kg and 200 kg. Note that, in the case of the 107 kg charge size where 27 examples were measured at NnG, it is possible to extrapolate a fit to the *measured* data to derive the exceedance ranges. Such a procedure gives values in between those of the UXO charge and the donor charge alone, for example giving a value of 3 km for peak sound pressure level for the VHF cetacean category (in comparison to the 5.7 km given from the model). The uncertainty in effective charge size and in the propagation will increase the uncertainty on the exceedance ranges. Another interesting observation here is that the weighted SEL is in many cases the determining factor, except for the HF group where the peak sound pressure level criterion seems to predict larger effect distances.

The general conclusion is that harbour porpoises, for example, are at risk of permanent threshold shifts at distances of several kilometres from large UXO detonations. The empirical data illustrated in Figs. 5 & 7 can also be used to inform consideration of marine mammal disturbance effects. In the UK for example, JNCC (2020, 2021) recommend a 26 km effective deterrence radius (EDR) for assessing the significance of noise disturbance from UXO clearance for conservation sites designated for harbour porpoise. Within this radius behavioral disturbance and habitat avoidance in harbour porpoises is predicted, extrapolating from the windfarm foundation piling data. For piling, this EDR has been considered somewhat conservative (*e.g.* Graham et al., 2019; Benhemma-Le Gall et al., 2021). Porpoise responses to single impulsive noise events such as UXO clearance by detonation are likely to be different to repetitive impulsive sound from piling.

The measured levels for the scare charges, though much lower in value than those for the UXO, are still reasonably high. The use of scare charges appears to be an attempt to facilitate a "ramp up" in radiated sound levels as advised in general guidance on other impulsive sources such as pile driving (JNCC, 2010) and airgun surveys (JNCC, 2017). Considering the levels obtained from the scare charges and their very short duration (which might provide limited information on source direction and therefore limited deterrent effect on marine mammals), the efficacy of their use as a deterrent should be established to justify the

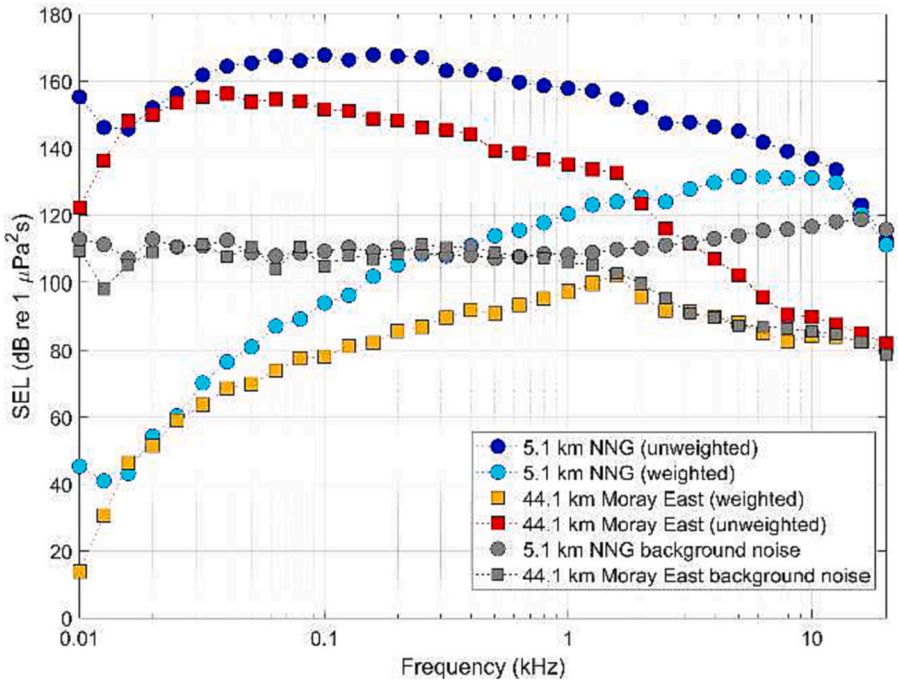

Fig. 16. Weighted (VHF species) and un-weighted measured SEL decidecade spectra at two of ranges for a 102 kg + 5 kg charge at NnG.

Table 3
Exceedance ranges for impulsive sound peak and weighted SEL for criteria from Southall et al., 2019.

Charge size (kg)	PTS Exceedance range (km)					
	peak			SEL (weighted)		
	LF	HF	VHF	LF	HF	VHF
1.0	0.3	0.08	1.6	0.3	0.06	2.1
5	0.6	0.2	2.5	1.0	0.08	4.1
10	0.6	0.2	2.9	1.3	0.1	5.2
100	1.4	0.5	5.7	4.5	0.3	9.9
200	1.7	0.6	7.1	6.1	0.4	10.2

additional loud impulsive noise they introduce to the environment. Note that, for the EOD campaigns at the two windfarms, ADDs were used before the scare charges in order to deter marine mammals in the area.

6. Conclusion

The study reported here represents the largest data set ever assembled for the assessment of noise radiated during UXO disposal. The UXOs studied here were mostly of fairly average size, with many of approximate size of 100 kg and only a few over 200 kg in size. Much larger charge sizes can be encountered in clearances of offshore windfarms.

The measurements were made at ranges of 1.5 km to 58 km from the UXOs. This is the first time that UXO detonations have been measured over such large ranges from the source, and the first time that scare charges (used in these cases for mitigation) have been measured. The large number of UXO detonations and scare charges enables the variations in the radiated sound to be assessed, and this is considerable. Agreement between predictions from a source and shallow-water propagation model and measurements show mixed results, with reasonable agreement obtained for one of the windfarms, but discrepancies obtained for the scare charges at the other windfarm, the results illustrating the inherent uncertainties in estimating the effective charge size and both modelling of the source and the shallow water propagation. The results obtained suggest that there is sometimes a doubt over how much of the UXO actually detonates, especially since some of measurements appear to be consistent with the levels for the donor charge alone. It seems likely that the seabed may reduce the radiated sound compared to that for a mid-water explosion. In general, the predictions of empirical scaling relations derived from mid-water models can overestimate the peak sound pressure and SEL in shallow water at large ranges.

The measurement and model results presented here confirm concerns that there can be injury and hearing effects at distances of several kilometres for large UXO detonations. It is therefore recommended that mitigation measures are adopted to reduce the risk of hearing impairment in receptors such as harbour porpoises. Mitigation measures include the use of spatial and temporal restrictions on the activity, passive acoustic monitoring to inform on the presence of animals, the use of Acoustic Deterrent Devices, and noise abatement technologies such as bubble curtains (Merchant and Robinson, 2020). Practical low-order alternatives for safely disposing of UXOs without full high-order detonations should also be explored (Robinson et al., 2020) and the authors recommend that further *in-situ* measurements be made of both low-order and high-order methods for comparison. It is recommended that the use of scare charges be critically examined for their efficacy as a deterrent to justify their use as mitigation considering the substantial additional impulsive noise they introduce into the environment.

CRediT authorship contribution statement

Stephen P. Robinson: Conceptualization, Methodology, Investigation, Writing – original draft. **Lian Wang:** Formal analysis, Investigation, Methodology. **Sei-Him Cheong:** Software, Investigation, Methodology. **Paul A. Lepper:** Conceptualization, Methodology, Investigation, Writing – review & editing. **John P. Hartley:** Writing – review & editing, Project administration. **Paul M. Thompson:** Conceptualization, Methodology, Investigation, Writing – review & editing. **Ewan Edwards:** Investigation, Writing – review & editing. **Michael Bellmann:** Investigation, Methodology, Writing – review & editing.

Declaration of competing interest

The authors declare that they have no known competing financial interests or personal relationships that could have appeared to influence the work reported in this paper.

Data availability

Data will be made available on request.

Acknowledgements

This project was funded by the UK's Department for Business, Energy and Industrial Strategy's Offshore Energy Strategic Environmental Assessment programme under contract OESEA-19-107. The authors would like to acknowledge Moray East and EDF Renewables and ESB, joint owners of NnG Offshore Wind, for use of their data. We also thank Moray First Marine for logistic support within the Moray Firth, and Tim Candido Barton, Ruth Molloy and Nathan Merchant for deploying recorders and processing acoustic data. The authors would also like to thank the anonymous reviewers for their insightful comments.

References

Ainslie, M.A., 2010. Principle of Sonar Performance Modelling. Springer, Chichester, UK.
Aker, J., Howard, B., Reid, M., 2012. Risk management for unexploded ordinance (UXO) in the marine environment. Dalhousie J. Interdiscip. Manag. 8. https://doi.org/10.5931/djim.v8i2.366. Available from: djim.management.dal.ca.
Albright, R.D., 2012. Chapter 6 -location, identification and environmental remediation. In: Cleanup of Chemical and Explosive Munitions, Second Edition. Elsevier, ISBN 9781437734775, pp. 71–98. https://doi.org/10.1016/B978-1-4377-3477-5.00006-4. In press.
Arons, A.B., 1954. Underwater explosion shock wave parameters at large distances from the charge. J. Acoust. Soc. Am. 26, 343–346.
Arons, A.B., 1970. Evolution of explosion pressure-wave characteristics in the region relatively close to origin. J. Acoust. Soc. Am. 47, 91.
BEIS, 2020. In: Cheong, S.-H., Wang, L., Lepper, P.A., Robinson, S.P. (Eds.), Protocol for In-Situ Underwater Measurement of Explosive Ordnance Disposal for UXO. Offshore Energy SEA Sub-Contract OESEA-19-107. Available from: link.
von Benda-Beckmann, A.M., Aarts, G., Sertlek, H.O., Lucke, K., Verboom, W.C., Kastelein, R.A., Ketten, D.R., van Bemmelen, R., Lam, F.A., Kirkwood, R.J., Ainslie, M.A., 2015. Assessing the impact of underwater clearance of unexploded ordnance on harbour porpoises (Phocoena phocoena) in the southern North Sea. Aquat. Mamm. 41 (4), 503–523.
Benhemma-Le Gall, A., Graham, I.M., Merchant, N.D., Thompson, P.M., 2021. Broad-scale responses of harbor porpoises to pile-driving and vessel activities during offshore windfarm construction. Front. Mar. Sci. 8, 664724 https://doi.org/10.3389/fmars.2021.664724.
Binnerts, B., de Jong, C.A.F., Karasalo, I., Östberg, M., Folegot, T., Clorenneq, D., Ainslie, M.A., Warner, G., Wang, L., 2019. Model benchmarking results for ship noise in shallow water. In: Proceedings of the 5th Underwater Acoustics Conference and Exhibition UACE2019, Hersonissos, Crete, Greece.
Chapman, N.R., 1985. Measurement of the waveform parameters of shallow explosive charges. J. Acoust. Soc. Am. 78, 672–681.
Chapman, N.R., 1988. Source levels of shallow explosive charges. J. Acoust. Soc. Am. 84, 697–702.
Cheong, S.-H., Wang, L., Lepper, P.A., Robinson, S.P., 2020. Characterisation of Acoustic Fields Generated by UXO Removal, Phase 2. Offshore Energy SEA Sub-Contract OESEA-19-107, NPL Report AC 19. Available from: link.
Cole, R.H., 1948. Underwater Explosions. Princeton University Press, Princeton, NJ.
Cooper, P.W., 1996. Explosives Engineering. Wiley-VCH. ISBN 0-471-18636-8.
Cristaudo, D., Puleo, J.A., 2020. Observation of munitions migration and burial in the swash and breaker zones. Ocean Eng. 205 https://doi.org/10.1016/j.oceaneng.2020.107322.
Croci, K., Arrigoni, M., Boyce, P., Gabillet, C., Grandjean, H., 2014. Mitigation of underwater explosion effects by bubble curtains : experiments and modelling, 14p. In: 23rd MABS (Military Aspects of Blast and Shock), Oxford, UK, Sep 2014, United Kingdom. https://hal.archives-ouvertes.fr/hal-01071652/.
Dahl, P.H., Jenkins, A.K., Casper, B., Kotecki, S.E., Bowman, V., Boerger, C., Dall'Osto, D. R., Babina, M.A., Popper, A.N., 2020. Physical effects of sound exposure from underwater explosions on Pacific sardines (Sardinops sagax). J. Acoust. Soc. Am 147 (4), 2383–2395.
Danil, K., St. Leger, J.A., 2011. Seabird and dolphin mortality associated with underwater detonation exercises. Mar. Technol. Soc. J. 45, 89–95. https://doi.org/10.4031/mtsj.45.6.5.
Davies, G., 1996. Munitions dump explodes into headlines again. Mar. Pollut. Bull. 32 (3), 250–251.
Detloff, K., Ludwichowski, I., Deimer, P., Schütte, H.-J., Karlowski, U., Koschinski, S., 2012. Environmental nongovernmental organizations' perspective on underwater munitions. Mar. Technol. Soc. J. 46 (1), 11–16.
Domenico, S.N., 1982. Acoustic wave propagation in air-bubble curtains in water—Part I: history and theory. Geophysics 47, 345–353. https://doi.org/10.1190/1.1441340.
Eitner, J., Tröster, S., 2018. Hazardous contaminated sites in the North and the Baltic Sea. Available from. In: Research News RN08. Fraunhofer Institute for Chemical Technology, Munich. www.Fraunhofer.de.
ESTCP, 2002. Report UX-0104, low-order underwater detonation, Environmental Security Technology Certification Program. Available from:. U.S. Department of Defense www.serdp-estcp.org/download/file/MM-0104.
Finneran, J.J., Jenkins, A.K., 2012. Criteria and Thresholds for U.S. Navy Acoustic and Explosive Effects Analysis. SSC Pacific, San Diego, CA. https://doi.org/10.21236/ADA561707.
Finneran, J.J., Schlundt, C.E., Carder, D.A., Clark, J.A., Young, J.A., Gaspin, J.B., 2000. Auditory and behavioral responses of bottlenose dolphins (Tursiops truncatus) and white whales (Delphinapterus leucas) to impulsive sounds resembling distant signatures of underwater explosions. J. Acoust. Soc. Am. 108, 417–431.
Gaspin, J.B., Shuler, V.K., 1972. Source levels of shallow underwater explosions. J. Acoust. Soc. Am. 51, 1202.
Gaspin, J.B., Goertner, J.A., Blatstein, I.M., 1979. The determination of acoustic source levels for shallow underwater explosions. J. Acoust. Soc. Am. 66, 1453–1462.
Graham, I.M., Merchant, N.D., Farcas, A., Barton, T.R., Cheney, B., Bono, S., Thompson, P.M., 2019. Harbour porpoise responses to pile-driving diminish over time. R. Soc. Open Sci. 6, 190335 https://doi.org/10.1098/rsos.190335.
Hamilton, E.L., 1980. Geoacoustic modeling of the seafloor. J. Acoust. Soc. Am. 68, 1313–1340.
Hannay, B., Chapman, N.R., 1999. Source levels for shallow underwater sound charges. J. Acoust. Soc. Am. 105 (1), 260–263.
Hayman, G., Robinson, S.P., Lepper, P.A., 2015. The calibration and characterisation of autonomous recorders used in measurement of underwater noise. Adv. Exp. Med. Biol. 875, 441–445. https://doi.org/10.1007/978-1-4939-2981-8_52, 11/2015.
Hayman, G., Robinson, S.P., Pangerc, T., Ablitt, J., Theobald, P., 2017. Calibration of marine autonomous acoustic recorders. In: IEEE OCEANS 2017, Aberdeen, pp. 1–8 doi: 0.1109/OCEANSE.2017.8084773.
ISO 18405:2017, 2017. Underwater Acoustics – Terminology. ISO (the International Organization for Standardization), Switzerland.
ISO 18406:2017, 2017. Underwater Acoustics – Measurement of Radiated Underwater Sound from Percussive Pile Driving. ISO (the International Organization for Standardization), Switzerland.
Jensen, F.B., Kuperman, W.A., Porter, M.B., Schmidt, H., 1997. Computational Ocean Acoustics. Springer (reprinted from 1994 AIP Press).
JNCC, 2010. JNCC guidelines for minimising the risk of injury to marine mammals from using explosives (August 2010). Available: www.jncc.gov.uk.
JNCC, 2020. Guidance for assessing the significance of noise disturbance against Conservation Objectives of harbour porpoise SACs (England, Wales & Northern Ireland). JNCC Report No. 654. ISSN 0963-8091. Joint Nature Conservation Committee, Peterborough. https://data.jncc.gov.uk/data/2e60a9a0-4366-4971-9327-2bc409e09784/JNCC-Report-654-FINAL-WEB.pdf.
JNCC, 2021. Impulsive noise in the Southern North Sea SAC (2015 to 2020). Joint Nature Conservation Committee final report to Defra. http://sciencesearch.defra.gov.uk/Document.aspx?Document=15220_JNCC2021_NoiseHpSACs_JNCC-Final.pdf.
JNCC, 2017. JNCC guidelines for minimising the risk of injury to marine mammals from geophysical surveys (August 2017). Available: www.jncc.gov.uk.
Ketten, D.R., Lien, J., Todd, S., 1993. Blast injury in humpback whale ears: evidence and implications. J. Acoust. Soc. Am. 94, 1849–1850. https://doi.org/10.1121/1.407688.
Kibblewhite, A.C., 1989. Attenuation of sound in marine sediments: a review with emphasis on new low-frequency data. J. Acoust. Soc. Am. 86, 716–738.
Koschinski, S., 2011. Underwater noise pollution from munitions clearance and disposal, possible effects on marine vertebrates, and its mitigation. Mar. Technol. Soc. J. 45 (6), 80–88.
Koschinski, S., Kock, K.H., 2009. Underwater unexploded ordnance - methods for a cetacean-friendly removal of explosives as alternatives to blasting. Reports Int. Whal. Comm. SC/61 E. https://literatur.thuenen.de/digbib_extern/dk041983.pdf.
Koschinski, S., Kock, K.H., 2015. Underwater unexploded ordnance - methods for a cetacean-friendly removal of explosives as alternatives to blasting. In: 22nd ASCOBANS Advisory Committee Meeting.
Loye, D.P., Arndt, W.F., 1948. A sheet of ar bubble as an acoustic screen for underwater noise. J. Acoust. Soc. Am. 20 (2), 143–145.
Merchant, N.D., Robinson, S.P., 2020. Abatement of underwater noise pollution from pile-driving and explosions in UK waters. In: Report of the UKAN Noise Abatement Workshop, 12 November 2019 at The Royal Society, London. https://doi.org/10.6084/m9.figshare.11815449.
Merchant, N.D., Andersson, M.H., Box, T., Le Courtois, F., Cronin, D., Holdsworth, N., Kinneging, N., Mendes, S., Merck, T., Mouat, J., Norro, A.M.J., Ollivier, B., Pinto, C., Stamp, P., Tougaard, J., 2020. Impulsive noise pollution in the Northeast Atlantic: reported activity during 2015–2017. Mar. Pollut. Bull. 152. https://doi.org/10.1016/j.marpolbul.2020.110951.
Moray East, 2011. Environmental Statement, Technical Appendix 3.4 A - Metocean and Coastal Processes Baseline. Moray Offshore Renewables Ltd doi: 0.1109/OCEANSE.2017.8084773.
NMFS, 2018. Revisions to technical guidance for assessing the effects of anthropogenic sound on marine mammal hearing. In: NOAA Technical Memorandum NMFS-OPR-59. US Dept. of Commer., NOAA. Available from: djim.management.dal.ca.

NnG, 2012. Environmental statement, chapter 8 - geology and bathymetry, Neart na Gaoithe Offshore Wind Farm. Available from: https://marine.gov.scot/data/environmental-statement-neart-na-gaoithe/.

NnG, 2021. Unexploded Ordnance – Underwater Noise Monitoring Report, NnG-NnG-ECF-REP-0033, Neart na Gaoithe Offshore Wind Farm. Available from: link.

NOAA, 2016. Available from www. In: Dahl, P., Ainslie, M. (Eds.), Independent Peer Review Reports of Underwater Calculator for Shocks. US National Ocean and Atmospheric Administration (NOAA), Center for Independent Experts. of Underwater Calculator for Shocks, or UWCv2 (Vers 2.0). https://www.st.nmfs.noaa.gov/science-quality-assurance/cie-peer-reviews/cie-review-2016.

Parsons, E.C.M., Birks, I., Evans, P.G.H., Gordon, J.C.D., Shrimpton, J.H., Pooley, S., 2000. The possible impacts of military activity on cetaceans in West Scotland. Eur. Res. Cetaceans 14, 185–190.

Popper, A.N., Hawkins, A.D., Fay, R.R., Mann, D.A., Bartol, S., Carlson, T.J., Coombs, S., Ellison, W.T., Gentry, R.L., Halvorsen, M.B., Løkkeborg, S., Rogers, P.H., Southall, B. L., Zeddies, D.G., Tavolga, W.N., 2014. Sound exposure guidelines for fishes and sea turtles: a technical report. In: ASA S3/SC1.4 TR-2014, ANSI Accredited Standards Committee S3/SC1, 2014. American National Standards Institute. https://doi.org/10.1007/978-3-319-06659-2.

Robinson, S.P., Lepper, P.A., Hazelwood, R.A., 2014. Good Practice for Underwater Noise Measurement. In: NPL Good Practice Guide No. 133. National Measurement Office, Marine Scotland, The Crown Estate. www.npl.

Robinson, S.P., Wang, L., Cheong, S.-H., Lepper, P.A., Marubini, F., Hartley, J.P., 2020. Underwater acoustic characterisation of unexploded ordnance disposal using deflagration. Mar. Pollut. Bull. 160, 111646.

Salomons, E.M., Binnerts, B., Betke, K., von Benda-Beckmann, A.M., 2021. Noise of underwater explosions in the North Sea. A comparison of experimental data and model predictions. J. Acoust. Soc. Am. 149 (3), 1878–1888.

Sayle, S., Windeyer, T.C.M., Conrod, S., Stephenson, M., 2009. Site assessment and risk management framework for underwater munitions. Mar. Technol. Soc. J. 43 (4), 41–51. https://doi.org/10.4031/MTSJ.43.4.10.

Schmidt, H., Jensen, F.B., 1985. A full wave solution for propagation in multilayered viscoelastic media with application to gaussian beam reflection at fluid-solid interfaces. J. Acoust. Soc. Am. 77, 813–825.

Schmidtke, E.B., 2010. "Schockwellendämpfung mit einem Luftblasenschleier zum Schutz der Meeressäuger", (Shock wave damping with an air bubble curtain to protect marine mammals). Berlin, March. In: Proceedings of DAGA 2010, pp. 689–690. http://pub.degaakustik.de/DAGA_2010/data/articles/000140.pdf.

Schmidtke, E.B., 2012. "Schockwellendämpfung mit einem Luftblasenschleier im Flachwasser", (Shock wave damping with an air bubble curtain in shallow water). In: Proceedings of DAGA 2012, pp. 949–950, 11/2015. http://pub.degaakustik.de/DAGA_2012/data/articles/000332.pdf.

SEA5, 2004. Seabed And Superficial Geology And Processes, Report of Strategic Environmental Assessment Area 5. UK Department of Trade and Industry.

Sertlek, H.O., Slabbekoorn, H., ten Cate, C., Ainslie, M.A., 2019. Source specific sound mapping: spatial, temporal and spectral distribution of sound in the dutch North Sea. Environ. Pollut. 247, 1143–1157.

Siebert, U., Stürznickel, J., Schaffeld, T., Oheim, R., Rolvien, T., Prenger-Berninghoff, E., Wohlsein, P., Lakemeyer, J., Rohner, S., Aroha Schick, L., Gross, S., Nachtsheim, D., Ewers, C., Becher, P., Amling, M., Morell, M., 2022. Blast injury on harbour porpoises (*Phocoena phocoena*) from the Baltic Sea after explosions of deposits of World War II ammunition. Environ. Int. 159, 107014 https://doi.org/10.1016/j.envint.2021.107014.

Skretting, A., Leroy, C.C., 1971. Sound attenuation between 200 hz and 10 kHz. J. Acoust. Soc. Am. 49, 276.

Soloway, A.G., Dahl, P.H., 2014. Peak sound pressure and sound exposure level from underwater explosions in shallow water. J. Acoust. Soc. Am. 136 (3), El218-223.

Southall, B.L., Finneran, J.J., Reichmuth, C., Nachtigall, P.E., Ketten, D.R., Bowles, A.E., Ellison, W.T., Nowacek, D.P., Tyack, P.L., 2019. Marine mammal noise exposure criteria: updated scientific recommendations for residual hearing effects. Aquat. Mamm. 45 (2), 125–232. https://doi.org/10.1578/AM.45.2.2019.125.

Sundermeyer, J.K., Lucke, K., Dähne, M., Gallus, A., Krügel, K., Siebert, U., 2012. Effects of underwater explosions on presence and habitat use of harbor porpoises in the German Baltic Sea. In: Popper, A.N., Hawkins, A. (Eds.), The Effects of Noise on Aquatic Life. Advances in Experimental Medicine and Biology. Springer, New York, NY, p. 730. https://doi.org/10.1007/978-1-4419-7311-5_64.

Todd, S., Stevick, P., Lien, J., Marques, F., Ketten, D., 1996. Behavioral effects of exposure to underwater explosions in humpback whales (Megaptera novaeangliae). Can. J. Zool. 74, 1661–1672.

Weston, D., 1960. Underwater explosions as acoustic sources. Proc. Phys. Soc. 76, 233–249.

Wiggins, S.M., et al., 2019. Seal Bomb Sound Source Characterization, MPL Technical Memorandum 633, Marine Physical Laboratory, Scripps Institution of Oceanography, University of California San Diego, La Jolla, CA. https://www.cetus.ucsd.edu/docs/reports/MPLTM633-2019.pdf. (Accessed 27 September 2022).

Winkler, K.W., Murphy III, W.F., 1995. Acoustic Velocity and Attenuation in Porous Rocks, Rock Physics and Phase Relations, A Handbook of Physical Constants. America Geophysical Union.

Yelverton, J.T., Richmond, D.R., Fletcher, E.R., Jones, R.K., 1973. Safe distances from underwater explosions for mammals and birds. In: Lovelace Foundation for Medical Education and Research, Albuquerque NM 87108, AD-766 952.